

N87-17949

TDA Progress Report 42-88

October–December 1986

Antenna Pointing Systematic Error Model Derivations

C. N. Guiar and F. L. Lansing

Ground Antenna and Facilities Engineering Section

R. Riggs

TDA Engineering Office

The pointing model used to represent and correct systematic errors for DSN antennas is presented. Analytical expressions are given in both azimuth-elevation (az-el) and hour angle-declination (ha-dec) mounts for RF axis collimation error, encoder offset, non-orthogonality of axes, axis plane tilt, and structural flexure due to gravity loading. While the residual pointing errors (rms) after correction appear to be within the ten percent of the half-power beamwidth criterion commonly set for good pointing accuracy, the DSN has embarked on an extensive pointing improvement and modeling program aiming toward an order of magnitude higher pointing precision.

I. Introduction

Since the beamwidth of the parabolic reflector antenna decreases with increasing aperture size and decreasing wavelengths, errors in pointing accuracy assume additional importance. The potential increase of gain is rapidly lost if the narrower beam is not directed at the target with acceptable accuracy. The antennas being used by NASA-JPL for deep space tracking at Goldstone (California), Spain, and Australia operate at the S (2.3 GHz) and X (8.4 GHz) frequency bands. For a 70-m antenna operating at these frequencies, this translates into half-power beamwidths of 128 and 35 millidegrees, respectively. In order to effectively utilize these antennas at these sizes and frequencies, one should be able to point the RF axis to within 10 percent of the half-power antenna beamwidth.

A pointing model is commonly used to represent and correct systematic errors that contribute to pointing inaccuracies. Systematic errors are repeatable errors that are not determined by chance but by a bias. Random (stochastic) errors remain

uncorrected and represent the “final” pointing system inaccuracy. This article describes the present mathematical model being used throughout the DSN and discusses possible future improvements for the model and the model-fitting process.

II. Sources of Systematic Pointing Error and System Overview

The antenna is commanded to point its beam axis at a (predicted) spacecraft location, referred to as a “predict” throughout the remainder of this article. The predicts are generated in the Antenna Pointing Assembly (APA), as shown in Fig. 1. Due to the many inherent pointing errors (systematic and random), the antenna boresight does not point to the desired point. Pointing corrections are therefore added to the predicted azimuth and elevation angles (or hour angle and declination angle) to compensate for the systematic portion of the pointing errors. These corrections are contained in the systematic error correction table of the Antenna Control Subassembly (ACS). Also located in the ACS are two other point-

ing corrections: (1) the refraction correction algorithm, which supplies an elevation correction based on temperature, humidity, and pressure values (Ref. 1) and (2) the "squint" correction table, which corrects for the boresight shift due to lateral motion of the subreflector. After the systematic, refraction, and "squint" corrections are added, the new command angles are sent to the Antenna Servo Controller (ASC) which generates the appropriate rate commands. During "blind" pointing, the shaft encoders send the feedback position signal for comparison with the command position signal. During spacecraft tracking and radio astronomy experiments, a different technique is used for closing in on the target whereby the antenna is scanned around its boresight in a circular pattern with a constant angular offset in order to detect the position of peak gain. This technique is referred to as conical scanning (con-scan) (Ref. 2).

The key sources of systematic pointing error to date can be itemized as follows (Refs. 3, 4, and 5): (1) RF collimation error, (2) encoder fixed offset, (3) axis skew, (4) azimuth axis tilt, (5) structural flexure due to gravity, and (6) residual refraction error. Each error will be further defined for the two types of DSN antenna mounts (the azimuth-elevation mount and the hour angle-declination mount) in the paragraphs that follow. The total error in pointing is expressed as the algebraic sum of the individual error source contributors. Noting that the amount of error from most of the above error sources is a function of the angular position of the antenna, the total error in each coordinate is computed accordingly.

The relevant coordinates for an Az-El mounted antenna are azimuth and elevation, the errors being expressed in ΔAz and ΔEl . For a polar mount antenna, the errors may be expressed as ΔHA and ΔDec . Using these coordinates, it can be shown that a fixed pointing error quantified in terms of ΔAz for an Az-El mount (or ΔHA for a polar mount) will vary with the elevation (or declination) angle of the beam. This occurs since the beam is never in the azimuth (or hour angle) plane except at zero elevation (or declination) angles. In order to avoid this difficulty, a coordinate system is used where the beam itself forms one axis, with the other two axes forming a plane orthogonal to the beam. For an Az-El mount, one axis is the elevation axis, the other is normal to the beam and is contained by the elevation plane. This will be referred to as the cross-elevation axis (Fig. 2). Pointing errors in this coordinate system may be expressed as

$$\text{Errors in the elevation plane} = \Delta El$$

$$\begin{aligned} \text{Errors in the cross-elevation plane} &= \Delta XEl \\ &= \Delta Az \times \cos(el) \end{aligned}$$

$$\text{Magnitude of total pointing error} \cong \sqrt{(\Delta El)^2 + (\Delta XEl)^2}$$

and for a polar mount antenna as

$$\text{Errors in the declination plane} = \Delta Dec$$

$$\begin{aligned} \text{Errors in the cross-declination plane} &= \Delta XDec \\ &= \Delta Ha \times \cos(Dec) \end{aligned}$$

$$\text{Magnitude of total pointing error} \cong \sqrt{(\Delta Dec)^2 + (\Delta XDec)^2}$$

III. Analysis of Systematic Errors

A. Azimuth (Hour Angle) Collimation Error

Collimation error is defined to be the nonorthogonality of the antenna beam to the elevation (or declination) axis. In order to derive an expression for collimation error, suppose a star is located at position X of the spherical system in Fig. 3 (Ref. 4) and the antenna is located in the center of the sphere. The antenna beam is displaced by an amount δ due to collimation error and points to position X' . The resulting azimuth error can be derived by solving spherical triangle WZX'

$$\begin{aligned} \cos(90 + \delta) &= \cos(90 - el) \cos 90 \\ &+ \sin(90 - el) \sin 90 \cos(90 + \Delta Az) \end{aligned} \quad (1)$$

which reduces to

$$-\sin \delta = \cos(el) \sin \Delta Az \quad (2)$$

If δ and ΔAz are small, Eq. (2) can be approximated by

$$\Delta Az = -\delta \sec(el) \quad (3)$$

When converted to XEl coordinates, the collimation error becomes

$$Xel = -\delta \quad (4)$$

There is no first order correction to elevation in the case of this azimuth collimation error.

Collimation error for a Ha/Dec-type mount is defined in the manner detailed above, with ha and dec replacing az and el , respectively.

B. Axis Skew

Axis skew is defined to be the nonorthogonality of the elevation (or declination) axis to the azimuth axis (or hour angle) axis. Figure 4 (Ref. 4) depicts the elevation axis skewness in the spherical system. The antenna is located in the center of the sphere with its azimuth and elevation axes

denoted by X_3 and X_2 , respectively. The axes are skewed by an amount ξ , so the antenna points to the displaced position S' instead of the star position S . The relationship between the skewed and nonskewed axes is given by

$$[X'] = [B] [X] \quad (5)$$

where $[B]$ is the transformation matrix and is given as

$$[B] = \begin{bmatrix} 1 & 0 & 0 \\ 0 & \cos\xi & -\sin\xi \\ 0 & \sin\xi & \cos\xi \end{bmatrix} \quad (6)$$

If ξ is small, $[B]$ becomes

$$[B] = \begin{bmatrix} 1 & 0 & 0 \\ 0 & 1 & -\xi \\ 0 & \xi & 1 \end{bmatrix} \quad (7)$$

Equation (5) expands into the following relationship

$$\left. \begin{aligned} X'_1 &= X_1 \\ X'_2 &= X_2 - X_3 \xi \\ X'_3 &= X_2 \xi + X_3 \end{aligned} \right\} \quad (8)$$

Axis skewness causes an error in both azimuth and elevation. The azimuth error due to skewness will be defined to be

$$\Delta Az = Az' - Az \quad (9)$$

For small values of azimuth error, Eq. (9) can be written as

$$\Delta Az = \tan Az' - \tan Az \quad (10)$$

where

$$\tan Az = \frac{X_2}{X_1} \quad (11)$$

and

$$\tan Az' = \frac{X'_2}{X'_1} = \frac{X_2 - X_3 \xi}{X_1} \quad (12)$$

The resulting ΔAz is

$$\Delta Az = -\frac{X_3}{X_1} \xi \quad (13)$$

Since X_3/X_1 is $\tan(el)$, the azimuth error resulting from axis skewness is

$$\Delta Az = \xi \tan(el) \quad (14)$$

or, in terms of XEl ,

$$\Delta XEl = \xi \sin(el) \quad (15)$$

The elevation error due to skewness is

$$\Delta el = \tan(el') - \tan(el) = \frac{X_2 \xi}{X_1} \quad (16)$$

which becomes

$$\Delta el = \xi \tan(\Delta Az) \quad (17)$$

Since the azimuth skewness is small, the skewness error in elevation will be small and can therefore be neglected.

Skew terms for a ha/dec-type mount are again defined in the same manner detailed above, with hour angle and declination replacing azimuth and elevation, respectively.

C. Azimuth (Hour Angle) Axis Tilt

Axis tilt is the deviation of the azimuth from the true vertical. For a polar mount, axis tilt is the deviation of the hour angle axis from the north celestial pole, or the amount of nonparallelism with the earth's spin axis. Figure 5 depicts X_1 as the neutral axis with ϕ being the angle at which the azimuth plane is tilted.

The azimuth error can be found by determining the rate of change of Q_K (which is the azimuth of the level axis (K_A) minus azimuth) with respect to the change in the magnitude of the X_2 coordinate

$$\begin{aligned} \Delta Az &= \frac{d(K_A - Az)}{dX_2} \Delta X_2 \\ &= \frac{d \left[\tan^{-1} \left(\frac{X_2}{X_1} \right) \right]}{dX_2} \Delta X_2 \end{aligned} \quad (18)$$

where $\Delta X_2 = X_2' - X_2$. The result of performing the differentiation is

$$\Delta Az = \frac{-X_1 d(X_2)}{[(X_2)^2 + (X_1)^2] dX_2} (X_2' - X_2) \quad (19)$$

The matrix to transform from an untilted coordinate system to a coordinate system tilted by an angle ϕ as given by $[x'] = [a] [x]$ is

$$[A] = \begin{bmatrix} 1 & 0 & 0 \\ 0 & \cos\phi & \sin\phi \\ 0 & -\sin\phi & \cos\phi \end{bmatrix} = \begin{bmatrix} 1 & 0 & 0 \\ 0 & 1 & \phi \\ 0 & -\phi & 1 \end{bmatrix} \quad (20)$$

if ϕ is small. One result of the matrix transformation is

$$X_2' - X_2 = (X_2 + X_3\phi) - X_2 = \phi X_3 \quad (21)$$

which changes Eq. (19) to

$$\begin{aligned} \Delta Az &= \frac{-X_1 d(X_2)}{[(X_2)^2 + (X_1)^2] dX_2} \phi X_3 \\ &= \frac{[\sin(K_A - Az)] \phi \rho \sin(el)}{\rho \cos(el)} \\ &= -\phi \tan(el) \sin(K_A - Az) \end{aligned} \quad (22)$$

The elevation error resulting from azimuth plane tilt is

$$\Delta el \cong \tan(el) - \tan(el') \quad (23)$$

Using the transformation matrix and the fact that

$$\tan(el) = \frac{X_3}{\rho \cos(el)} \quad (24)$$

$$\tan(el') = \frac{X_3'}{\rho \cos(el)} \quad (25)$$

then

$$\begin{aligned} \Delta el &= \frac{X_3}{\rho \cos(el)} - \frac{-\phi X_2 + X_3}{\rho \cos(el)} = \frac{\phi X_2}{\rho \cos(el)} \\ \Delta el &= \phi \cos(K_A - Az) \end{aligned} \quad (26)$$

Tilt terms for a ha/dec-type mount are also defined in the same manner detailed above, with hour angle and declination replacing azimuth and elevation, respectively.

D. Structural Flexure Due to Gravity

Forces due to gravity result in moments upon the structure, deflecting the truss members and panels, thus changing the shape of the antenna. These forces and moments change directions and magnitude with the elevation angle. Due to the gravitational deformation of the structure, the antenna beam is deflected relative to the shaft encoder on the elevation axis.

The antenna structural error under gravity loading is computed as the algebraic sum of the individual errors, each caused by a single structure component under one type of deformation (e.g., translation and rotation). The three key structural components considered are the main reflector, the subreflector, and the feed cone. The five individual errors of interest as shown in Fig. 6 are main reflector axis rotation, main reflector vertex translation, subreflector vertex translation, subreflector axis rotation, and feed translation.

Each element of deformation could generate a boresight pointing error in space about the x -axis ($\Delta\theta_x$) and about the gravity y -axis ($\Delta\theta_y$). Due to the almost symmetrical antenna geometry about the y - z plane $\Delta\theta_y$ is negligible and only the pointing errors $\Delta\theta_x$ are considered. The total pointing error under gravity loading about the x -axis is expressed as the

$$\sum_j \theta_x(j)$$

Geometrical factors are introduced for each type of deformation to translate the component into an antenna rf beam error (Ref. 6).

Each error component $\Delta\theta_x(j)$ can be represented as the resultant effect of pointing errors at the true extreme elevation positions:

$$\begin{aligned} \Delta\theta_x(j) &= \Delta\theta_x^y(j)[\cos(el) - \cos(\alpha_r)] \\ &\quad + \Delta\theta_x^z(j)[\sin(el) - \sin(\alpha_r)] \end{aligned} \quad (27)$$

where α_r is the antenna-panel setting (rigging) elevation angle (usually 45 degrees), $\theta_x^y(j)$ is the rotation about the x -axis due to weight loading applied parallel to the reflector y -axis and $\theta_x^z(j)$ is the rotation about the x -axis due to weight loading applied parallel to the reflector z -axis (Refs. 7 and 8). These two loading conditions provide sufficient information to compute the structural pointing error at any elevation angle of the antenna.

For a ha/dec-type mount the az/el expression for flexure given in Eq. (27) is converted to ha/dec coordinates using the identities of spherical trigonometry, resulting in (Refs. 9 and 10)

$$\Delta HA = -\sin(ZD) \sin(\beta) - X'_c \quad (28)$$

$$\Delta DEC = -\sin(ZD) \cos(\beta) - Y'_c \quad (29)$$

where ZD is the zenith angle (90 degrees - el), β is the paraxial angle, X'_c is the component value of the surface panels setting angle and Y'_c is the component value of the surface panel declination angle. The pointing correction in terms of $xdec$ is

$$\Delta xdec = [-\sin(ZD) \sin(\beta) - X'_c] \cos(dec) \quad (30)$$

Other flexure corrections are included to compensate for subreflector position error. Due to deformation of the main reflector, the foci of the main reflector and subreflector do not coincide. The subreflector offset (in inches) required to accommodate this condition is

$$y - \text{offset} = 3.41 [\sqrt{2} \cos(el) - 1] \quad (31)$$

and is part of the Subreflector Controller (SRC) software. A correction is also made for the boresight shift due to the lateral motion of the subreflector, "squint" correction, is

$$\text{"squint" correction} = (y - \text{offset}) \frac{(M-1)R}{MF} \quad (32)$$

where

M = magnification factor of the subreflector

R = reflection ratio

F = focal length

The squint correction algorithm is located in the ACS.

E. Residual Error Due to Refraction

The residual pointing error is the resultant error that remains after the "standard" corrections (Ref. 1) for bending are made in the refraction correction algorithm of the ACS. At the present time, the correction for the residual pointing error is made using the following expression

$$\Delta el = K \cot(el) \quad (33)$$

where K is the constant that takes into account the residual effects of temperature, pressure, and humidity.

IV. Pointing Model Generation

A pointing model is used to characterize the various sources of pointing error for the antenna and consists of the items detailed in the previous section. An az-el antenna will be used in this section to demonstrate the methodology involved in the usage and development of new models.

The equation for the elevation and cross-elevation pointing offsets are

$$\begin{aligned} \Delta Xel &= P1 + P2 \cos(el) \\ &+ P3 \sin(el) \\ &+ P4 \sin(el) \cos(az) \\ &+ P5 \sin(el) \sin(az) \end{aligned} \quad (34)$$

$$\begin{aligned} \Delta el &= -P4 \sin(az) \\ &+ P5 \cos(az) + P7 \\ &+ P8 \cos(el) + P9 \cot(el) \end{aligned} \quad (35)$$

where

$P1 = \delta$, the magnitude of collimation axis misalignment

$P2 =$ azimuth encoder fixed offset

$P3 = \xi$, elevation axis skew angle

$P4 = -\phi \sin K_A$ (ϕ is the azimuth axis offset and K_A is the azimuth of the level axis)

$P5 = \phi \cos K_A$

$P7 =$ elevation encoder fixed offset and elevation collimation error

$P8 = \Delta\theta_x^y$, the antisymmetry loading pointing error computed for a hypothetical horizon position ideal cassegrainian antenna under unit gravity off/on loading

$P9 = K$ (residual refraction error)

Initially, pointing offset data were collected for various conscan tracks using a program called CAPTURE. Approximately every two seconds, this program reads the azimuth and elevation angles, azimuth and elevation offsets, and time tags the data. The azimuth offset is next converted to XEL coordinates, so it can be entered into the model fitting program (acronym PHO). The PHO program uses a linear least-squares technique to fit the offset data to the functions given in Eqs. (34) and (35). The least squares fit determines the parameters P_i . The systematic error correction table can then be generated and loaded into the Antenna Pointing Assembly

(APA) and then into the ACS. These past efforts resulted in sets of parameters to be used for specific tracks.

V. Conclusion

Figures 7 and 8 demonstrate the effect of model corrections by showing a set of offset data before and after corrections are made. The plots show the offsets after correction are within 10 percent of the half-power beamwidth.

So far, the pointing effort is concentrating on improving and verifying the pointing model and adjusting those initially developed parameter sets. The measurable parameters (i.e., tilt, orthogonality, etc.) of Eqs. (34) and (35) will be field

verified and a Fourier analysis will be performed to ensure that no more systematic errors are present and only random errors remain. When it is determined that the selected set of parameters are acceptable and all of the systematic errors seem to be accounted for, alternate methods of fitting the offset data to the functions of Eqs. (34) and (35) will be examined.

Secondly, since conscan data sets were initially collected and identified with specific tracks, many systematic error correction models are presently being used. It is believed that these models can be condensed into one model representing error corrections over the entire sky. Finally, a technique will be studied to update these models in a timely fashion as new offset data are collected.

References

1. Berman, A. L., and Rockwell, S. T., "New Optical and Radio Frequency Angular Tropospheric Refraction Models for Deep Space Applications," *JPL Technical Report 32-1601*, Jet Propulsion Laboratory, Pasadena, Calif., November 1975.
2. Ohlson, J. E., and Reid, M. S., "Conical Scan Tracking with the 64 m Diameter Antenna at Goldstone," *NASA Technical Report 32-3605*, Jet Propulsion Laboratory, Pasadena, Calif., October 1976.
3. Meeks, M. L., Ball, J. A., and Hull, A. B., "The Pointing Calibration of the Haystack Antenna," *IEEE Trans. on Ants. and Prop.*, *AP-16*, No. 6, pp. 746-751, November 1968.
4. Burak, M., "Pointing Calibration of a High-Resolution Millimeter-Wave Antenna by Star Observations," *Air Force Systems Command AFCRL-71-0220*, Air Force Cambridge Research Laboratories, March 1971.
5. Stumpff, P., "Astronomical Pointing Theory for Radio Telescopes," *Klein-heubacher Berichte*, *15*, pp. 431-437, 1972.
6. Isber, A. M., "Obtaining Beam-Pointing Accuracy With Cassegrain Antennas," *Micro-waves*, *6*, No. 8, pp. 40-44, August 1967.
7. Katow, M. S., and Mori, M., "Computation of RF Boresight Direction from Reflector Distortions," *JPL Technical Report 32-1526, XVII*, pp. 78-82, Jet Propulsion Laboratory, Pasadena, Calif. 1973.
8. Katow, M. S., "64 m Diameter Antenna: Computations of RF Boresight Direction," *JPL Technical Report 32-1526, XIV*, pp. 68-72, Jet Propulsion Laboratory, Pasadena, Calif., 1973.
9. Katow, M. S., and Levy, R., "Computation of Gravity RMS for HA-DEC Antennas," *DSN Progress Report 42-27*, pp. 139-147, Jet Propulsion Laboratory, Pasadena, Calif., 1975.
10. Katow, M. S., "34-Meter Antenna-Subreflector Translations to Maximize RF Gain," *TDA Progress Report 42-62*, pp. 112-120, Jet Propulsion Laboratory, Pasadena, Calif., 1981.

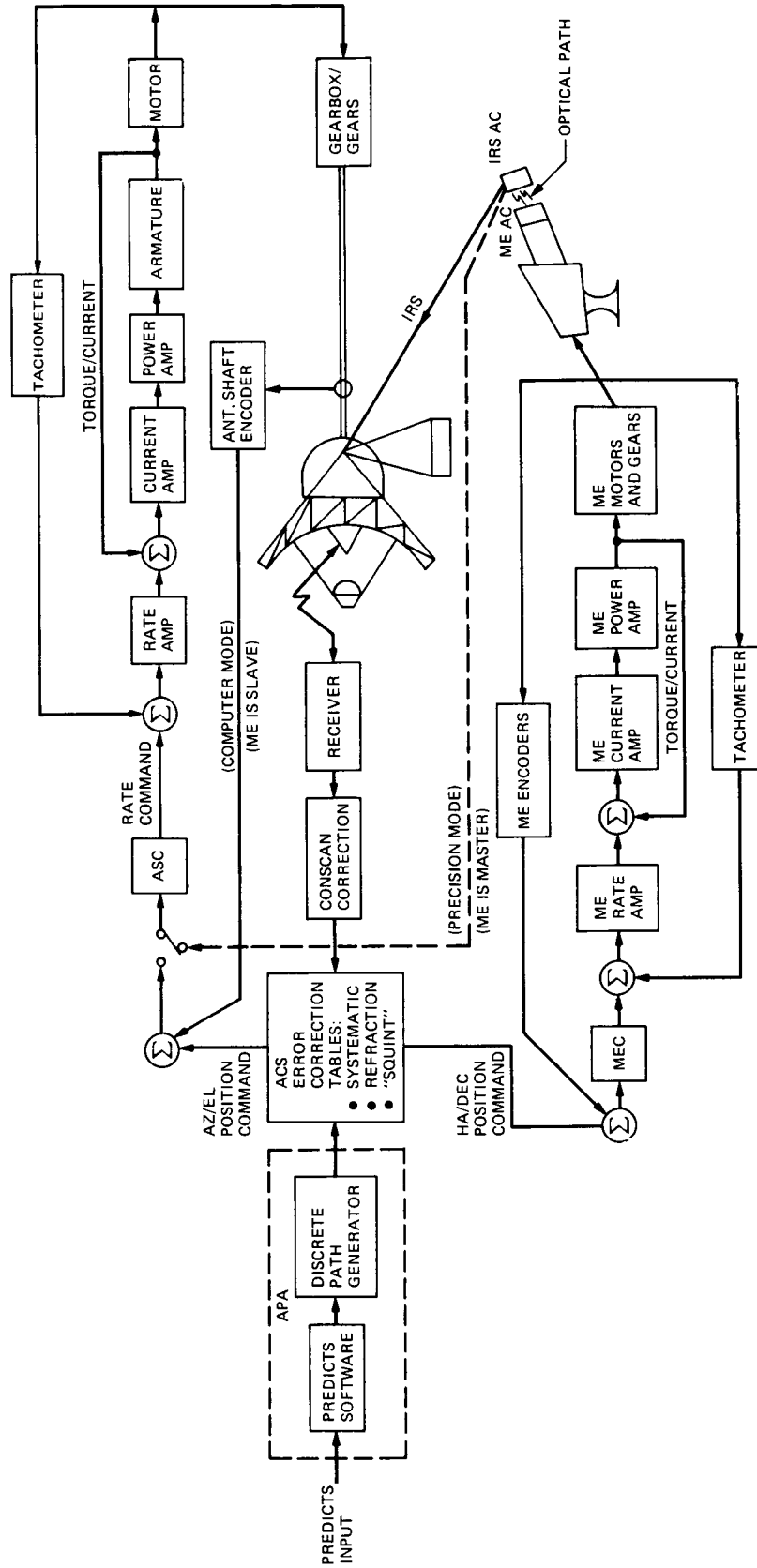
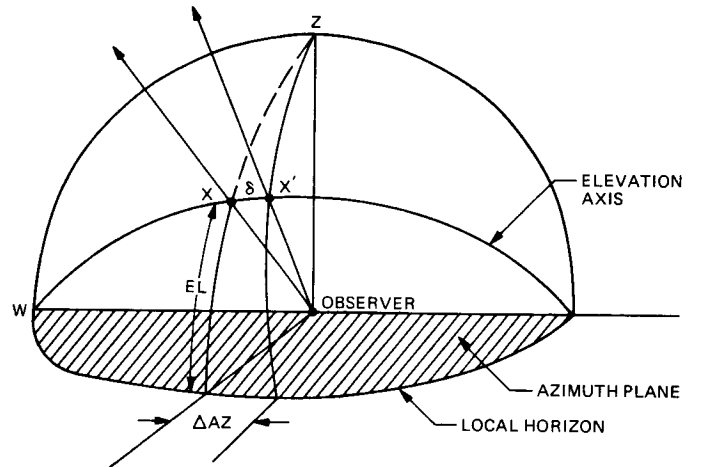
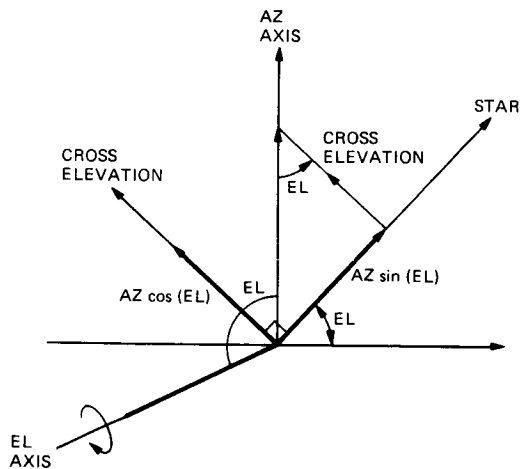
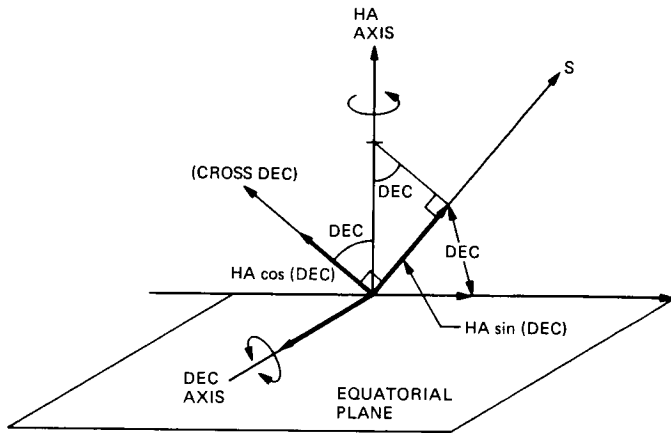


Fig. 1. Overview of the antenna pointing system



X = STAR POSITION
 X' = DISPLACED ANTENNA BEAM
 δ = MAGNITUDE OF COLLIMATION AXIS MISALIGNMENT
 ΔAZ = AZIMUTH ERROR
 Z = LOCAL ZENITH

Fig. 3. Azimuth collimation error

Fig. 2. Azimuth-elevation and hour-angle declination coordinate systems showing cross elevation and cross-declination axes, respectively

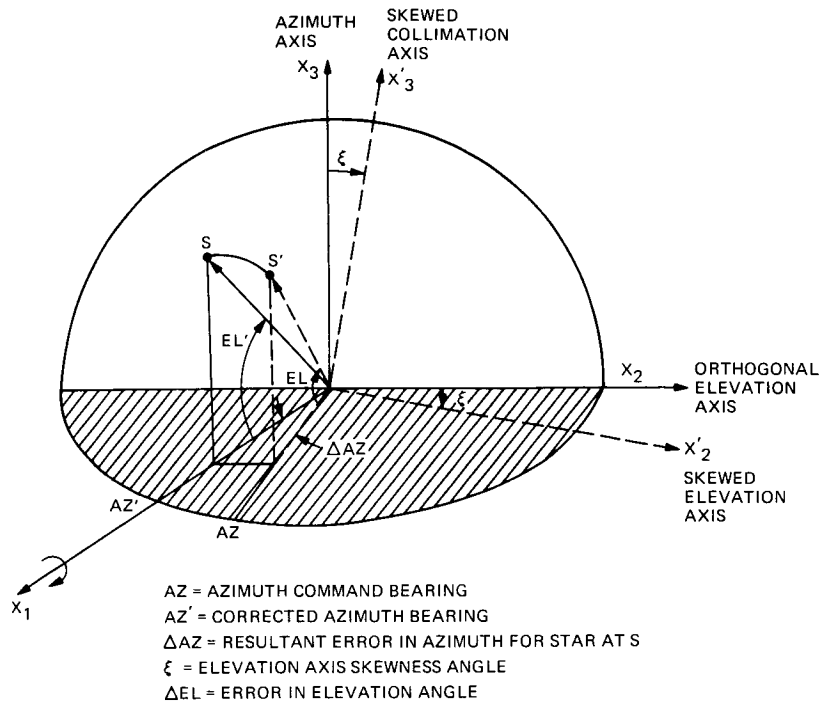


Fig. 4. Elevation axis skewness

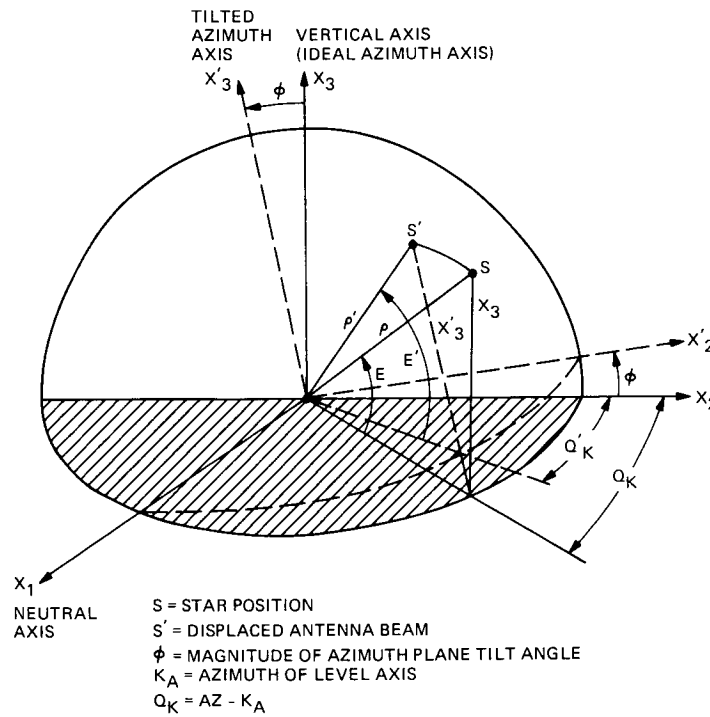


Fig. 5. Azimuth plane tilt

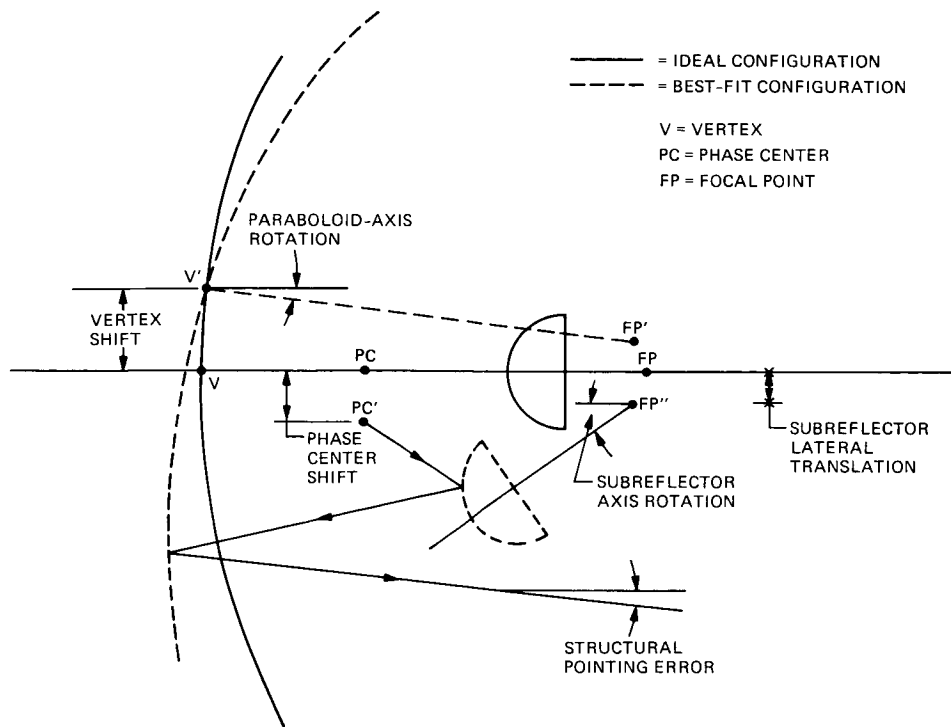


Fig. 6. Structural feed misalignments

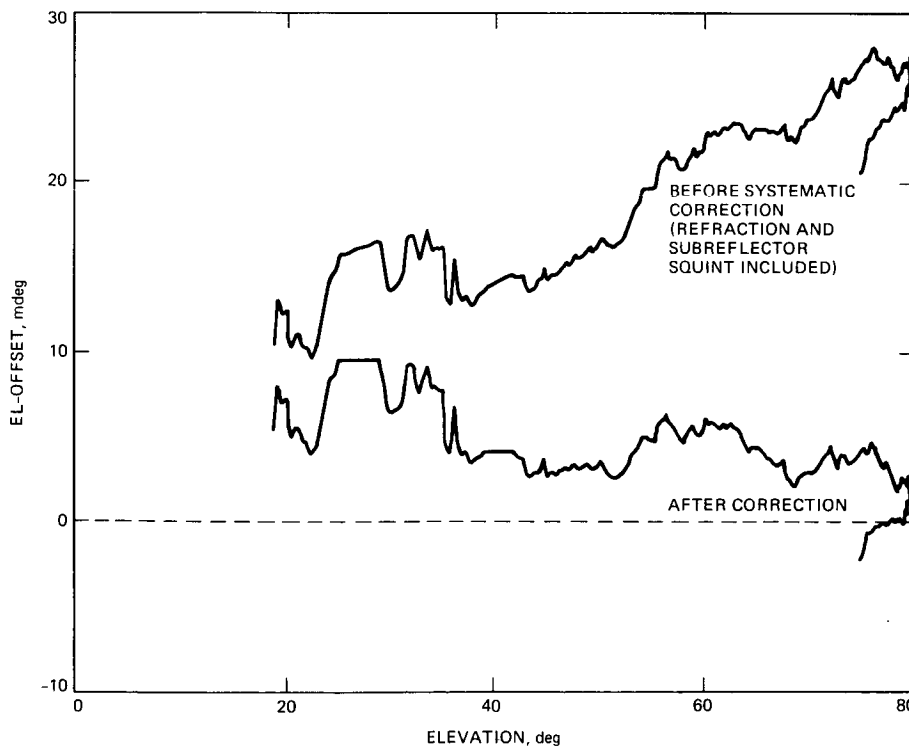


Fig. 7. Elevation vs *EL*-offset before and after systematic error correction, Mars, 64-m antenna

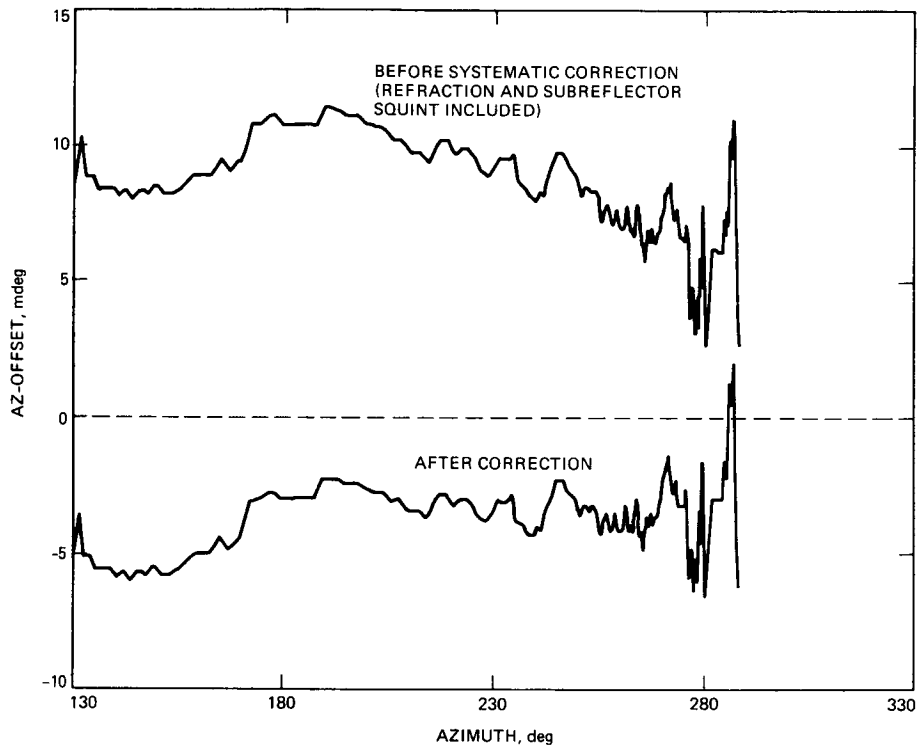


Fig. 8. Azimuth vs AZ-offset before and after systematic error correction, Mars, 64-m antenna